PAPER

Investigating temperature influences on shell growth and microstructural variations in bay scallops: insights from multiscale microscopy

Benazir Khurshid, [ID] *[a] Arnaud Benchetrite,[a] Lise Guichaoua, [ID] [b] Nicolas Brodusch, [ID] [b] Bryce D. Stewart, [ID] [cd] Roland Kröger, [ID] [e] Raynald Gauvin, [ID] [b] Martin Mallet,[f] Réjean Tremblay [ID] [g] and Natalie Reznikov [ID] *[ahi]

Scallops (order Pectinida) are well-known for their robust and beautiful calcitic shells that protect them from external impacts and predators. Scallops respond to environmental conditions, including water temperature, salinity, and food supply, which are reflected in the shell growth rates and patterning. The bay scallop (*Argopecten irradians*) is a species of high ecological and aquacultural value in North America, and its habitat may expand towards higher latitudes with inevitable global warming. To investigate the effect of water temperature on the accretion rate and the polycrystalline microstructure of the Bay scallop shell, we conducted a controlled growth experiment on juveniles, 4 weeks following their larval metamorphosis. Approximately 400 individuals, collected from a hatchery 4 weeks after metamorphosis, were then reared in reconstituted seawater for 9 weeks at 23 °C and 26 °C. At 7-, 9-, 11-, and 13-weeks post-metamorphosis, calcein was added to the water for 7 hours for fluorescent staining, and then equal batches of scallops were collected and fixed. Morphologic characterization of bay scallop shells included micro-computed X-ray tomography for 3D measurements to measure shell thickness, and fluorescence light microscopy for accretion rate assessment. We used mechanical testing of complete shells in compression to assess their stiffness, strength and toughness. Microstructural analysis of the shells included

[a]Department of Bioengineering, McGill University, Canada. E-mail: natalie.reznikov@mcgill.ca; benazir.khurshid@mcgill.ca

[b]Department of Mining and Materials, McGill University, Canada

[c]Marine Biological Association, UK

[d]School of Biological and Marine Sciences, University of Plymouth, UK

[e]School of Physics, Engineering and Technology, University of York, UK

[f]Huîtres Mallet Inc., Canada

[g]Institut des Sciences de la mer, Université du Québec à Rimouski, Canada

[h]Department of Anatomy and Cell Biology, McGill University, Canada

[i]Faculty of Dental Medicine and Oral Health Sciences, McGill University, Canada

scanning electron microscopy and crystallographic analysis by electron backscattered diffraction. The scallops reared in warmer water exhibited a faster growth rate with shells showing higher calcite grain misorientation, no difference in relative shell thickness, and inconclusive difference in the shell mechanical properties. This study may help us to understand the multifarious implications of climate change.

Introduction

Scallops belong to the molluscan family Pectinidae that comprises approximately 350 extant species. Scallops date back to the Mesozoic and Cenozoic eras, showcasing immense diversity in morphology, behavior, and biology.[1,2] They survived two mass extinction events over the past 245 million years.[1,2] Scallops now provide significant quantities of seafood through a variety of commercially important fisheries and aquaculture initiatives around the world.[3]

Most commercially valuable scallop species inhabit inshore waters of continental shelves, although they can also be found at depths ranging from the intertidal zone to approximately 7000 meters, highlighting their adaptability and ecological versatility.[4] The bay scallop (*Argopecten irradians*), for instance, live in shallow bays and estuaries with salinity 15–30 psu, and are frequently found in eelgrass beds, where young scallops attach to eelgrass blades using thin byssal threads.[5] This species is distributed along the eastern coast of the United States, from Cape Cod, Massachusetts, to the Laguna Madre in southern Texas, extending into northeastern Mexico.[6] With changing climate conditions, their geographic range is expected to expand northward.

Bay scallops are hermaphroditic, with external fertilization occurring in the water column or on the seabed, where male gametes are generally released before female gametes to reduce the likelihood of self-fertilization. Spawning typically occurs in warmer months. Fertilized eggs hatch into free-swimming embryos, which develop into pelagic veliger larvae with a small shell.[7] After undergoing metamorphosis, larvae become benthic spats and begin developing adult features and filter-feed on plankton. Juveniles grow quickly, acquiring their distinctive shell and mobility, and can move around by clapping their shells to evade predators. Within 6 to 12 months, they reach adulthood.

The bay scallop's two shell valves are nearly identical in shape and flare (Fig. 1). These valves are rounded with prominent ribs (plicae) radiating from the central, wing-like umbo.[6] As the scallop grows, distinct concentric growth lines form along the shell's edge, normal to the plicae. The bottom (or right) valve is slightly more convex than the top ("left") valve. The right valve features a notch for the foot and anchoring byssus threads, decorated by a series of small knobs known as the ctenolium along the notch's ventral margin (Fig. 1). The shell mineral is deposited by a thin organ called the mantle, within the extrapallial space enclosed by the mantle, the periostracum (the outermost shell layer), and the growing shell edge.[8,9] Calcium and bicarbonate ions from water or food are absorbed by the inner mantle epithelium, the gills, and the digestive system. These ions are then transported to the outer epithelium *via* the hemolymph and extruded into the extrapallial space, where the transition from liquid precursors to solid crystalline mineral occurs.[9] This process of shell deposition results in the bay scallop shell's distinct structure, which primarily consists of
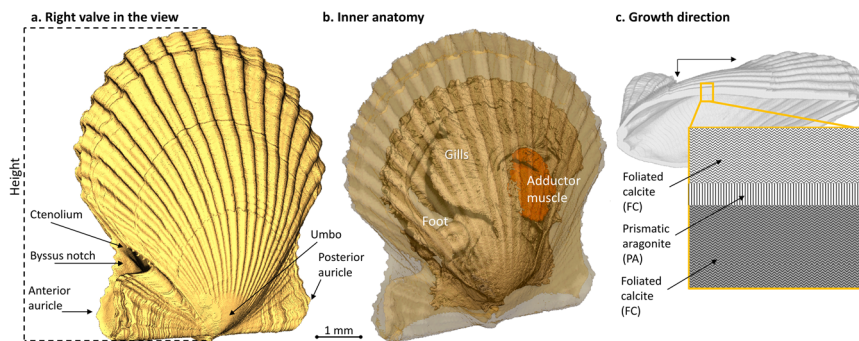
Fig. 1 Scallop shell morphology and valve features (a), and inner anatomy (b), imaged by microcomputed tomography (μCT), and (c) schematic of calcium carbonate layered structure when the shell is cut longitudinally.

calcitic foliated layers, with a thin layer of aragonitic prismatic pallial myostracum.[10,11] The foliated calcite layers, made up of submicrometer-thin calcitic laths arranged in a three-dimensional polycrystalline weave, enable scallops to rapidly mineralize and efficiently thicken their shells.[9,12] In contrast, the pallial myostracum is composed of elongated, regular aragonite prisms. This complex 3D architecture of scallop shells enhances their toughness and provides effective protection.

Scallops are effective indicators of environmental conditions, recording changes in temperature, salinity, food abundance, and water quality within their shells,[13,14] manifested in shell growth rates and patterning. A recent study demonstrated that heavy metal runoff pollutants can compromise the toughness and strength of the King Scallop (*Pecten maximus*) shell.[15] Similarly, temperature is a factor influencing shell accretion, with reports showing higher shell growth rates with increasing temperatures and an optimal temperature range for bay scallops of around 15 to 27 °C.[16] While research has linked shell growth to environmental factors, ultrastructural studies focusing specifically on the effect of water temperature on shell microstructure are relatively scarce.[17] As climate change increasingly changes the temperature of the world's oceans, understanding the effects of such changes on the structural integrity of scallops, and therefore their resistance to predation and disturbance, is becoming increasingly important.

Since scallops are poikilotherm animals (organisms whose internal body temperature varies with the surrounding environment), their metabolic rate follows the ambient temperature. Hence, the first hypothesis was whether the shell mineral accretion rate increases with temperature. One secondary aim of this study was the assessment of possible structural changes in the shells when scallops were grown at cool and warm temperatures, and the consequences for shell robustness.

Results

Shell growth

As scallop shells grow, they maintain consistent proportions – a small shell looks like a scaled-down replica of a large shell, and their morphology can be described by a few relatively simple parameters.[18–20] Therefore, plotting only one linear
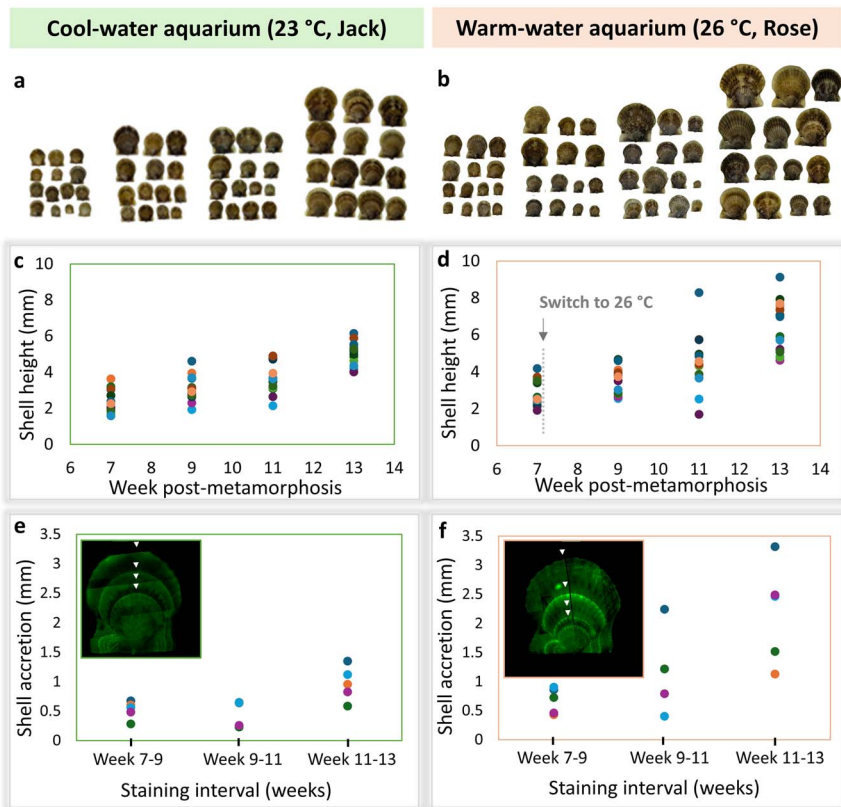
Fig. 2 Shell size and growth rate in different rearing conditions. Overview of the sampled groups (a and b) shows notable biological variation in size. Plots of shell height of 14 scallops per group harvested at weeks 7, 9, 11, and 13 post-metamorphoses from aquaria maintained at 23 °C (c) and 26 °C (d). Plots of three shell height increments in scallops grown in cool (e) and warm water (f), between the four staining events, 5 individuals per group. The shell growth increments were measured perpendicular to two adjacent fluorescent lines (Calcein staining). Insets in e and f show mosaic fluorescence micrographs with the growth lines indicated by white arrowheads.

dimension, such as height, is indicative of the shell growth trends in other dimensions. Fig. 2 shows that in both cool and warm water lab aquaria, there are smaller and larger shells, consistent with their natural variation. Following the temperature increase from 23 to 26 °C in one aquarium (referred to as "warm"/ Rose) at week 7 post-metamorphosis, the scallops in this group acquired larger linear sizes. This trend reached statistical significance ($p = 0.0043$) by week 13 (Fig. 2c and d). Individual variation in response to higher temperature was notable. This is consistent with the changes in the accretion rate, indicated by the three intervals between adjacent fluorescent labels (four labels in total; Fig. 2e and f). In the first interval, before the temperature was increased in the warmer tank, the shell accretion rate was similar between the two groups, averaging less than 0.5 mm per week. Following the temperature increase, a difference in shell accretion rate was observed. In the second interval, scallops in the cooler 23 °C

aquarium exhibited either the same or reduced shell accretion over two weeks compared to the first interval, while those in the warmer aquarium showed an increased growth rate, up to 2 mm in two weeks. Although the second interval showed a higher variation in the accretion rate in warmer water, only at the third interval was the difference statistically significant ($p = 0.018$). The upward trend in the accretion rate was accompanied by the increase in the variation within the group.

Shell thickness

The differences in the shell proportions and relative thickness were compared by acquiring the 3D volume of scallop shells using X-ray microtomography (μCT). Obviously, a smaller shell would be thinner than a larger shell, and to enable quantitative comparisons of the shell proportions, all the μCT-imaged shells were digitally resized to normalize local thickness to height to assess whether one group of shells was 'lankier' (thinner) or 'burlier' (thicker) than the other group. Fig. 3 shows the original sizes of the shells rendered in uniform colours, next to the thickness maps of the same specimens digitally re-sized to the largest one (top pink shell b(i) in a dashed frame). While the warmer water shells appear larger (Fig. 3b) and more diverse in size, the local thickness maps illustrate two trends. Firstly, in both groups the auricles and the radial ridges are thicker (warmer, yellow-green colour) than the rest of the shell. Secondly, the warmer water shells show not only higher variation in their absolute sizes, but also a higher variation in proportions (Fig. 3b). Note that shells (ii) and (iii) in Fig. 3b were both small within their group (~4 mm), but Shell 2 was the 'lankiest', and Shell 3 was the 'burliest'. Statistical analysis of the thickness map measurements is presented as overlapping histograms in Fig. 3c. There is no statistical difference in the normalized local shell thickness between the groups.

Shell strength

As the lack of morphological differences may or may not manifest as similar mechanical competence of the shells, we conducted mechanical testing of the shells collected at week 11 post-metamorphosis, using compression. Fig. 4 shows strength (force at failure), stiffness (slope of the force–displacement curve in the linear region prior to failure), and toughness (area under the force–displacement curve, representing the energy required to break the specimen).

Although absolute strength and toughness were higher in the warm group, the difference in vanishes after normalization by shell weight. The normalized strength was somewhat higher in the warm group ($p = 0.0154$) but it remains inconclusive whether the difference is biologically significant since the sample size was small, 8 shells per group.

Shell microstructural and crystallographic features

To analyze the microstructure of the shell, we inspected Epon-embedded, longi-tudinally cut and polished specimens using scanning electron microscopy (SEM) and a backscattered electron (BSE) detector. BSE imaging is sensitive to specimen composition and shows a mineral crystallites' boundaries. To identify the calcium carbonate polymorphs, *i.e.* calcite and aragonite, to assess their relative
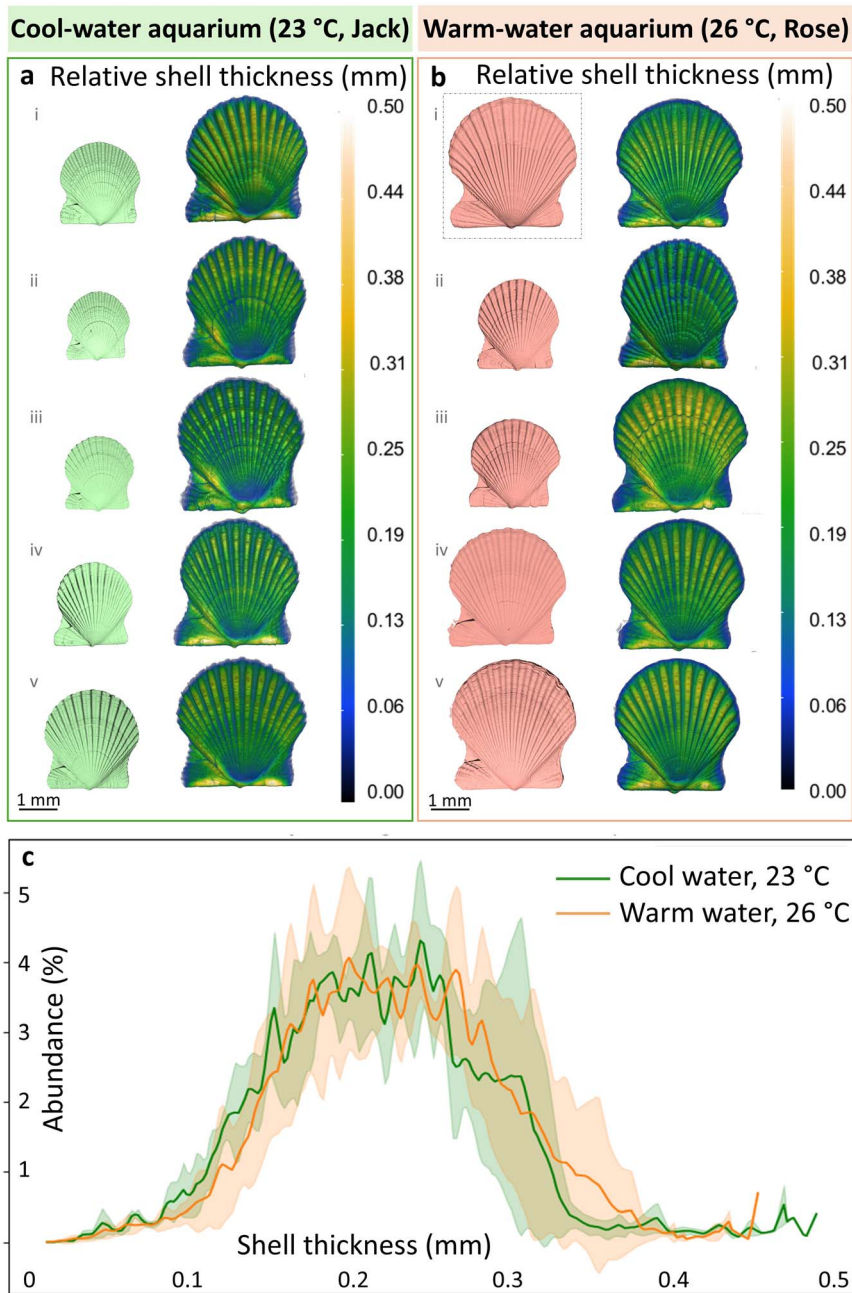
Fig. 3 Shell thickness measurements of scallops grown in cool (a) and warm (b) water. In panels a and b, the left column illustrates the original sizes of the shells, and the right column shows normalized shell thickness (thickness map) of five scallops from week 13 post-metamorphosis. The thickness values are normalized to the height of the largest shell from the warm aquarium (panel b, dashed frame) and are color-coded. (c) Overlay of average profiles of scallop shell thickness distributions from two temperature groups (23 °C in green and 26 °C in pink). Solid lines represent the mean abundance of local thickness values for each group, while the shaded areas indicate ±1 standard deviation.
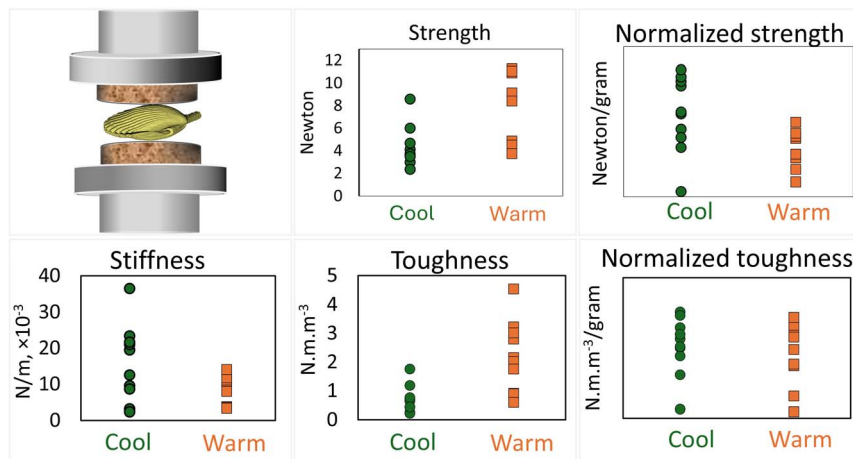
Fig. 4 Micromechanical testing of 4 complete shells per group in compression. Strength and toughness are presented as absolute values and normalized by the shell weight. Stiffness is shown only as absolute values. The shells were selected to be approximately of the same size of ~4–5 mm. Cool-water shell weight varied between 0.006–0.018 g; warm-water shell weight varied between 0.018–0.039 g.

crystallinity, and to map the crystallographic orientation of grains, electron backscattered diffraction (EBSD) was used. One 13 weeks specimen from each aquarium (cool and warm) was imaged at multiple magnifications, and then crystallographic analysis was performed in the shell middle region where aragonite myostracum is sandwiched between foliated calcite bulk layers (Fig. 5). The hinge region is the oldest shell area, accrued prior to the water temperature increase in the warm aquarium – its features are presented in Fig. 6. The distal tip of the shell is the most recently deposited area, accrued 6 weeks after the water temperature increase in the warm aquarium, and it is shown in Fig. 7.

Foliated-prismatic layer. In the middle section (Fig. 5), both the pallial myo-stracal layer and the bulk of foliated calcite are visible. The prismatic layer in both groups had a thickness of around 40–50 μm and showed a banding pattern likely related to the shell growth cycles. In the cool-water specimen, the overall crystallinity and/or grain size appeared to be lower in both prismatic and foliated layers (Fig. 5c, band contrast map). The polymorphs of both the prismatic and foliated layers in both groups were confirmed by the phase map acquired using EBSD at a pixel resolution of 170 nm, with blue representing calcite and red representing aragonite (Fig. 5b). The Inverse Pole Figure (IPF) color map in Fig. 5d illustrates the preferential orientation of crystallographic planes with respect to the normal to the sample surface. For example, the aragonitic prismatic layer in both groups showed alternating domains with {010} and {100} planes (green and blue) being normal to the sample surface. In both cases, the crystal domains towards the outer layer are better indexed compared to those near the inner layer due to the difference in grain sizes.

The foliated layer in the plane-of-section seems to have different orientations in cool and warm water shells. As has been described, folia are composed of adjacent, blade-like laths. In both specimens, the EBSD maps show that the
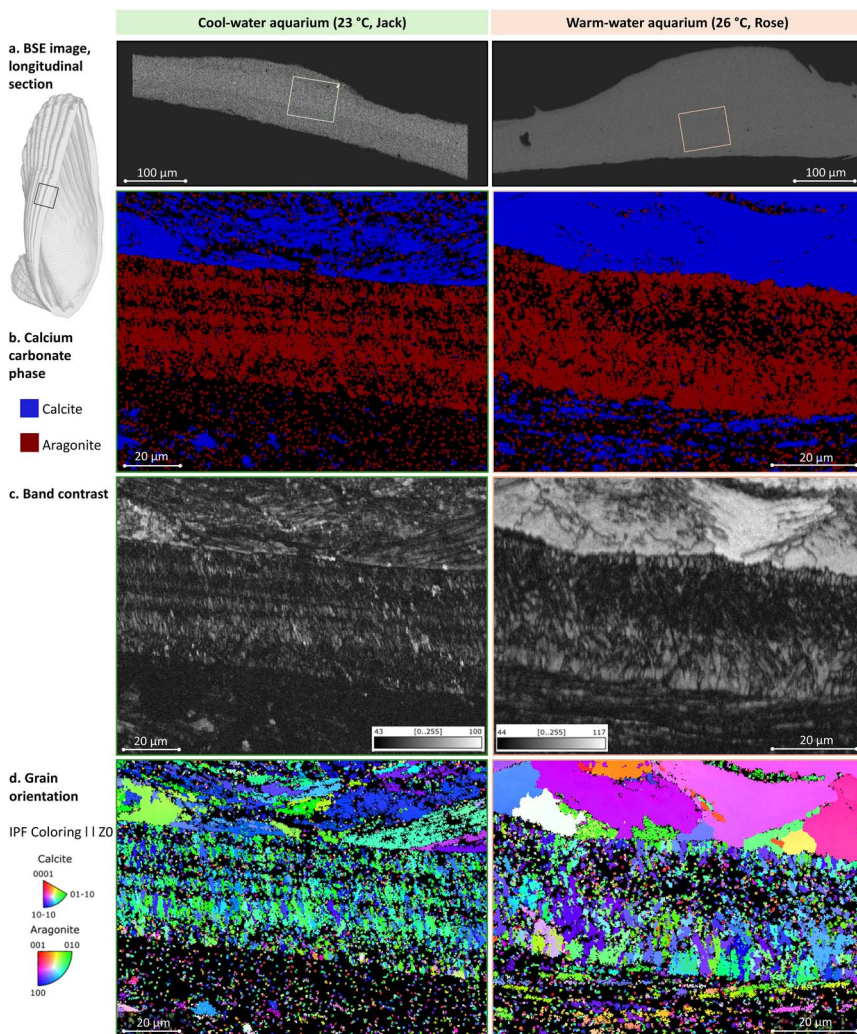
Fig. 5   Microstructure and crystallographic analysis of the middle portion of the shell's longitudinal section in scallops grown in cool (left panel) and warm (right panel) water. (a) Backscattered electron (BSE) images of the middle portion of the shell cross-section. The rectangles in each image denote the areas selected for EBSD analysis. (b) EBSD phase map highlighting two layers: the foliated layer composed of calcite (blue) and the prismatic layer composed of aragonite (red). (c) EBSD band contrast image of the shell cross-section from both groups, illustrating the microstructure and texture of calcite and aragonite in the foliated and prismatic layers, respectively. (d) EBSD Inverse Pole Figure (IPF) coloring map showing the orientation of calcite and aragonite crystals in the foliated and prismatic layers, respectively.

foliated calcite towards the outer side of the prismatic layer shows higher index values, while many pixels towards the inner side remain unassigned (black). In the case of the warm-water specimen, the crystal domains of the folia on the outer side of the prismatic layer are larger and more homogeneous compared to the crystal domains of the folia in the cool-water specimen. Moreover, the

crystallographic orientation of the foliated layer on the outer side of the prismatic layer differs between the cool- and warm-water specimens, with the cool-water specimen displaying a somewhat monotonous orientation of smaller domains (blue and green orientations, Fig. 5d, left), while the warm water specimen showing a more diverse orientation of larger and locally homogeneous domains (Fig. 5d, right).

Hinge area. In the hinge area, in both cool-water and warm-water specimens, the calcitic laths sections are 1–2.5 μm wide and 250–300 nm thick, separated by ∼20 nm grain boundaries that contain organic matter (appear dark in the micrographs, Fig. 6a). The visual, qualitative difference in grain size and grain boundary thickness between the cool and warm specimens can be attributed to the 2D nature of the image of a 3D structure. Volumetric BSE imaging using focused ion beam-scanning electron tomography (FIB-SEM) would be helpful to quantify the microstructure objectively. There is no appreciable difference in the crystallinity (Fig. 6c), polymorph distribution (Fig. 6b) and grain orientation in the hinge region (Fig. 6d).

Growing edge. In the growing distal tip of the shell, the shape of the calcitic laths were irregular in both specimens, and they were not as tightly packed in the foliated layer as compared to the foliated layer near the hinge (Fig. 7a). Additionally, presumably organic material was present between the calcitic laths, evident as dark areas in Fig. 7a. The abundance of organic matter between the grains is indeed expected in immature shell regions.[21] The EBSD maps show that the foliated calcite in the warm water specimens is more completely indexed, while many pixels remain unassigned (black) in the cool-water specimens. This could be attributed either to the presence of more organics in the cool-water specimens, or to the grain size, or to factors entirely dependent on specimen preparation, such as the flatness of the sample. In the cool-water specimen, the calcite crystal orientation (Fig. 7d, left) was similar to that observed near the hinge (Fig. 6d, left). However, in the warm-water specimen, the crystal orientation in this region (Fig. 7d, right) differs from the orientation near the hinge (Fig. 6d, right), with dominant orientations in red, pink, light blue, and green, covering a larger range of grain orientations.

Pole figures illustrating the texture of polycrystalline calcite in the middle of the shell longitudinal section, in the hinge region and in the growing distal tip area are shown in Fig. 8. The contoured pole figures provide statistical data on crystallographic texture in the middle of the shell, hinge and tip areas (from Fig. 5–7) measured in Multiple of Uniform Distribution (MUD) values derived from the maxima of the pole figures. A higher MUD value reflects a stronger local texture.

In *Argopecten irradians*' shells from both cool and warm aquariums, a coherent crystallographic preferred orientation of the calcite [0001] and aragonite [001] axes was observed in all three regions (Fig. 8). The MUD values of the foliated calcite layer varied across these regions. In the middle section, the warm-water specimens exhibited a higher MUD value (49.30) compared to the cool-water specimens (33.97), indicating stronger calcite co-orientation (Fig. 8a and b), or higher crystallinity of co-oriented domains, or larger domains. Conversely, aragonite showed higher MUD values in the cool-water specimens than in the warm ones (Fig. 8c and d), perhaps attributable to the stronger co-orientation of similarly sized aragonite grains.
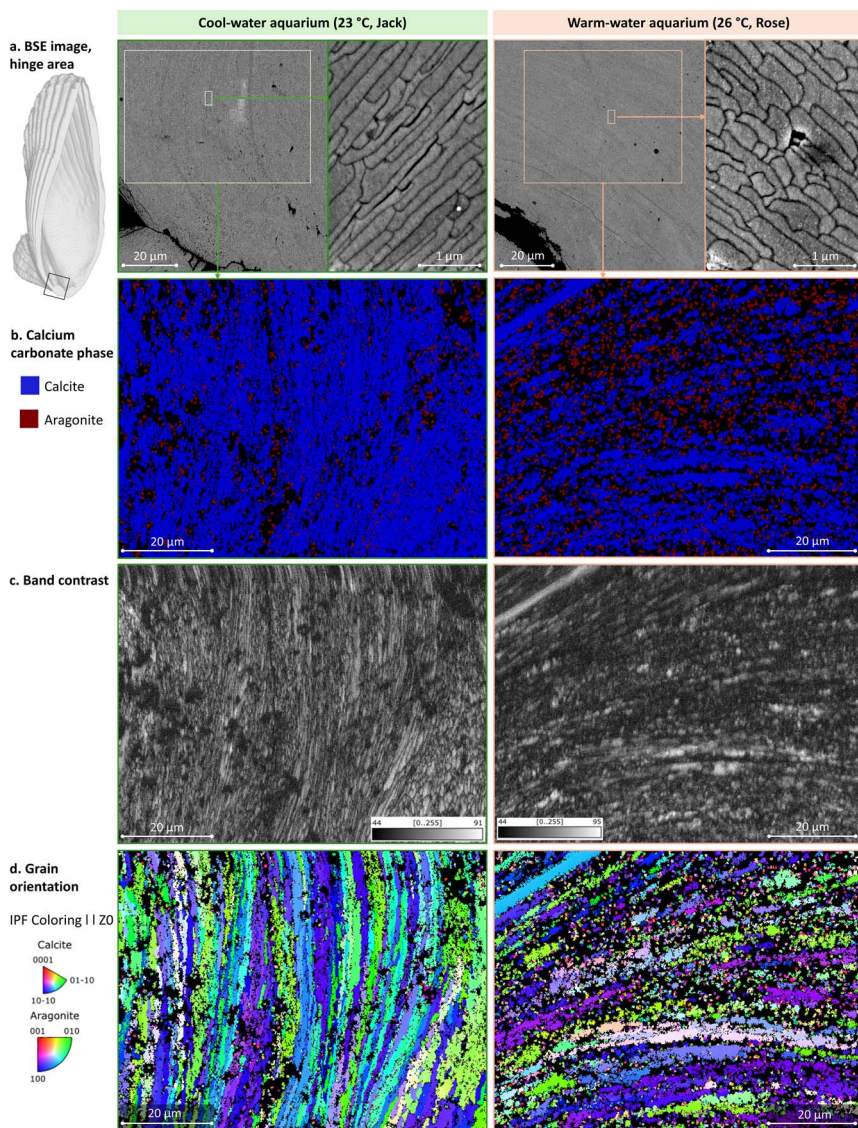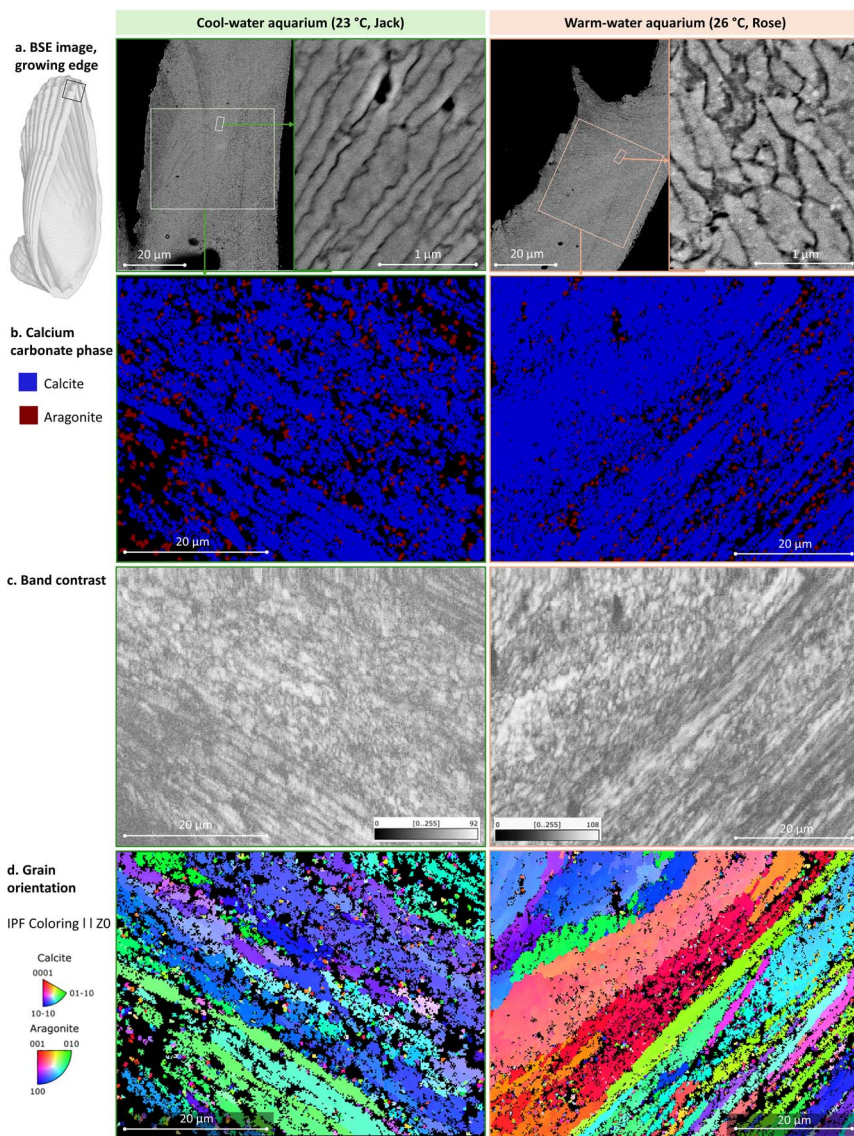
Fig. 6 Microstructure and crystallographic analysis near the hinge of the shell cross-section of scallops grown in cool (left panel) and warm (right panel) water. (a) Back-scattered electron (BSE) images of the shell cross-section. Insets show the BSE images at higher magnification of the area marked with small rectangles, showing the laths arranged into a foliated layer surrounded by organics (dark). The large rectangles in each image denote the areas selected for EBSD analysis. (b) EBSD phase map confirming the layer is made of calcite (blue). (c) EBSD band contrast image of the shell cross-section from both groups, illustrating the microstructure and texture of calcite in the foliated layer. (d) EBSD Inverse Pole Figure (IPF) color map showing the orientation of calcite in the foliated layer.

In the hinge area, formed before the temperature was increased in the warm aquarium, the MUD values remained similar between the two specimens (Fig. 8e and f), consistent with observations from the IPF color maps (Fig. 6d). However, at

Fig. 7 Microstructure and crystallographic analysis in the growing distal tip of the shell cross section of scallops grown in cool (left panel) and warm (right panel) water. (a) Backscattered electron (BSE) images of the shell cross-section. Insets show the BSE images at higher magnification of the area marked with small rectangles, showing the irregular shaped laths arranged into a foliated layer surrounded by organics (dark). The large rectangles in each image denote the areas selected for EBSD analysis. (b) EBSD phase map confirming the layer consists of calcite (blue). (c) EBSD band contrast image of the shell cross-section from both groups, illustrating the microstructure and texture of calcite in the foliated layer. (d) EBSD Inverse Pole Figure (IPF) coloring map showing the orientation of calcite in the layer.

the growing edge, a significant difference was evident between warm and cool water specimens, with lower MUD values in the warm water specimen indicating stronger calcite misorientation (Fig. 8g and h).
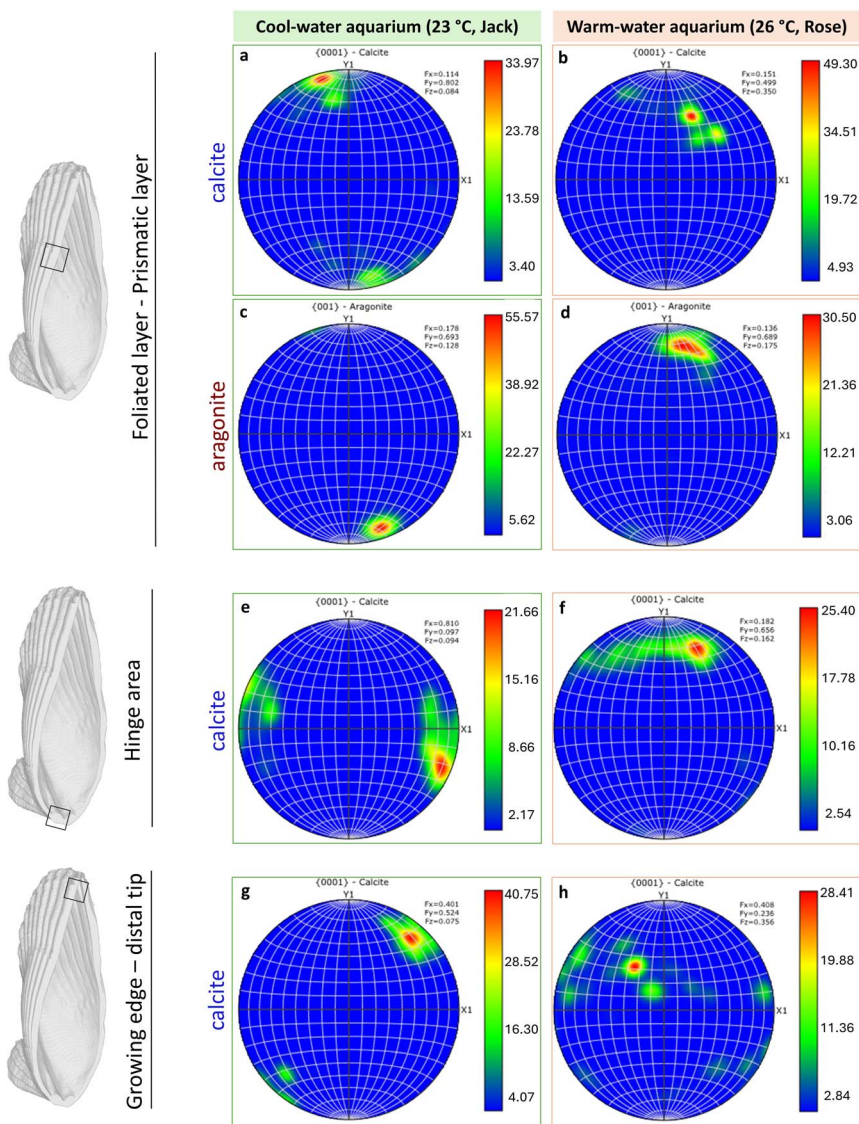
Fig. 8 Pole figures for calcite and aragonite representing the entire orientation maps shown in Fig. 5(d), 6(d) and 7(d). Scale is given in Multiple of Uniform Distribution (MUD).

Discussion

The findings of this study indicate that bay scallops (*Argopecten irradians*) grow faster in moderately warmer water, consistent with findings for other bivalve species.[17,22] Shell formation is a biologically mediated process where organic macromolecules form a supramolecular template for calcium carbonate precipitation.[23] This template dictates the size, shape, and orientation of microstructural units, becoming part of the biomineral as the intercrystalline organic matrix.[24,25] The synthesis of these macromolecules is linked to metabolic rate,

which is influenced by temperature and food quality.[26] In this poikilothermic organism, warmer ambient temperatures elevate metabolic rates, increasing organic matrix production and transmembrane pump activity, enhancing the delivery of Ca^{2+} and HCO_3^- to calcification sites.[27] Moreover, elevated temperatures may enhance enzymatic activity and protein synthesis, contributing to faster shell growth. Increased temperatures can accelerate the turnover rate of calcium-binding proteins and enzymes involved in biomineralization, further boosting the calcification process. However, while increased temperatures can accelerate the turnover rate of calcium-binding proteins and enzymes involved in biomineralization, this effect may only persist up to a threshold of 27–29 °C, beyond which high mortality ensues, for example, in *Mytilus edulis* that inhabits a similar latitude range as *A. irradians*.[28,29] Although short exposure to >30 °C can be tolerated,[29] beyond 40 °C, irreversible protein denaturation occurs in non-thermophilic species.

The variation in shell height and thickness we observed between scallops reared in cold- and warm-water conditions also reflected differences in growth rates. Higher variation in linear size, accretion rate, and local normalized thickness under warmer conditions, suggests an increase in total variation by expanding away from the minimal value, consistent with the constraint paradigm presented by Gould.[30] This finding of the population distribution diverging away from a limit, conspicuously follows the Maxwell–Boltzmann distribution in statistical mechanics, where increasing temperature causes the energy distribution of 'particles' to spread out and flatten, rather than shift bodily to the right, attaining both higher mean value and higher variance. Scallops, being poikilothermic organisms with a metabolic rate following the ambient temperature (to a certain limit) and diffusion rate, apparently literally adhere to the Maxwell–Boltzmann distribution in the studied temperature range. Indeed, no life form is exempt from the laws of thermodynamics.[31]

The exponential growth of linear dimensions in both cold and warm water, possibly reflecting the logarithmic flare of the shell edge, is expected to eventually plateau[32] upon reaching maturity. A longer-term experiment could help determine the shape of the bay scallop growth curve, and its response to temperature.

Changes in crystallography and microstructure of scallop shells between cold and warm water conditions were observed in this study using SEM and EBSD. While the microstructural differences were not distinctly evident in the 2D imaging, EBSD measurements revealed differences in the orientation of calcite and aragonite grains between the two groups. Our findings suggest that warmer conditions may induce subtle changes in the organization and orientation of calcite crystals. Notably, we observed difference in the MUD values, indicating higher misorientation in the distal growing tip of a warm water specimen compared to one from cool water. The exact correlation between this misorientation and the accelerated shell growth rate remains unclear to us. However, slight misorientation of adjacent crystallites has been proposed to enhance shell toughness through mechanisms such as crack deflection, branching, and the formation of tortuous paths that slow crack propagation.[33] This hypothesis could be confirmed by future studies employing nanoindentation techniques to measure local toughness and assess the impact of misorientation on mechanical properties – as has been demonstrated in different species of bryozoans.[34] Moreover, understanding the precise 3D changes in microstructural units, such

as calcitic laths and prisms, could be achieved through FIB-SEM volume acqui-
sition. To obtain a comprehensive view of crystal orientation distribution and to
better characterize the effects of temperature on shell biomineralization, 3D
EBSD would also be essential. These advanced methodologies would provide
deeper insights into how warmer conditions influence the structural and
mechanical properties of scallop shells, and future studies to this effect are in
progress.

Warming and ocean acidification are critical drivers of global change that by
altering ocean chemistry and temperature, impose energetic constraints on
marine organisms, affecting their survival.[35–37] Thus, we hypothesized that
warmer temperatures could impair shell strength and robustness, making them
more vulnerable to threats such as storms, dredging and predation. However, our
findings did not reveal any striking difference in shell strength or shell thickness
between the two groups. This suggests that *Argopecten irradians* may have
mechanisms to maintain shell integrity under warmer conditions, at least within
the range tested in our experiments. One possible explanation is that the organic
matrix proteins within the shell, which are crucial for reinforcing shell structure,
continue to function effectively despite the accelerated shell growth at a moder-
ately higher temperature. These proteins may help compensate for any potential
weakening effects caused by rapid calcification, thereby maintaining shell
mechanical competency. Contrary to our results in scallops, some research has
indicated that elevated temperatures can lead to thinner or weaker shells in other
bivalve species.[38,39] This discrepancy might be attributable to the fact that *A.
irradians* is a warmth-adapted species.[40] The difference in outcomes might be due
to species-specific adaptations or the experimental conditions, which warrant
further investigation. Additionally, the interplay between temperature and other
environmental factors, such as pH levels, could have complex effects on shell
formation and strength. In terms of ecological implications, the ability of bay
scallops to sustain shell quality in warming waters could be advantageous for
their survival, reducing their vulnerability to predation. This resilience might
indicate a potential for adaptation to climate change, although long-term studies
are necessary to confirm this. We acknowledge that our experiment's relatively
short duration might limit the observation of long-term effects of temperature on
shell robustness and strength. Future research should focus on extended periods
to capture the full life cycle of scallops and explore the molecular mechanisms
underlying shell robustness in varying environmental conditions.

In discussing the outcomes of our study, it is important to acknowledge the
limitations. Firstly, the study design was exploratory (post-hoc), as no effect size
prediction could be made, no statistical power was calculated, and the sample
size was based on the laboratory capacity. The results of this exploratory experi-
mental design can direct us towards more robust, preplanned statistical analyses.
Secondly, while controlled environments allow for precise manipulation of vari-
ables such as temperature, they inevitably lack the complexity and variability of
natural habitats. Factors such as water flow, natural diet, predator presence, and
other environmental interactions are not fully replicated in a laboratory setting.
Consequently, both groups of scallops may have experienced impediments in
growth and shell development compared to their natural counterparts. Previous
research has shown that other scallop species (*Pecten maximus*) of cultured origin
exhibited microstructural modifications more frequently than those from wild

populations, particularly in older individuals.[41] These findings suggest that the aquaculture environment can influence the biomineralization process, potentially leading to abnormalities over time. Future studies should consider integrating more natural setups or field studies to gain a comprehensive understanding of how bay scallops respond to environmental variations in their native ecosystems.

Conclusions

This study explored the effects of warmer water on the growth, microstructure, and mechanical properties of bay scallop (*Argopecten irradians*) shells. Our findings addressed three hypotheses as follows:

• Faster shell growth: the shells exhibited accelerated growth in warmer water, consistent with the influence of elevated temperatures on metabolic and biomineralization rates in poikilothermic organisms.

• Crystallographic differences: while no significant microstructural changes were observed, EBSD measurements revealed differences in the orientation of calcite and aragonite crystals, particularly higher misorientation in the distal growing tip of the warm-water specimen.

• Shell robustness and strength: despite the accelerated growth, there was no striking difference in shell robustness or strength between the two groups, suggesting the presence of compensatory mechanisms, such as the continued functionality of organic matrix proteins.

These findings highlight the resilience of *Argopecten irradians* under moderately warmer conditions, while underscoring the need for further research into long-term effects, species-specific adaptations, and the interplay of environmental stressors on shell biomineralization.

Methods

Rearing bay scallops: experimental conditions

The effects of water temperature on the growth and shell microstructure of juvenile bay scallops (*Argopecten irradians*) were examined through an experiment conducted over a 9 week period from May to July 2024 (weeks 4–13 post-metamorphosis). Scallop spats, measuring 1 mm in shell height at four weeks after metamorphosis, were obtained from a commercial hatchery (Huîtres Mallet Inc. https://www.malletoyster.com/) in Shippagan, New Brunswick, Canada. Groups of 200 scallops were transferred to each of two 30-liter glass aquaria (30 cm length × 26 cm width × 50 cm height), filled with reconstituted seawater with a salinity of 27–28 ppt (Instant Ocean Sea Salt, Instant Ocean). A light : dark regime of 12 : 12 hours was maintained using timer-controlled white light.

For the first two weeks, both tanks were kept at a constant temperature of 23 °C. Subsequently, during weeks 7–13 post-metamorphosis the temperature in one tank was increased to 26 °C (Aquarium Rose, orange-pink labels and frames in the figures), while the other remained at 23 °C (Aquarium Jack, mint-green labels and frames in the figures) to investigate the impact of warmer temperature on the scallops' growth and shell microstructure. The scallops were fed three times daily with a mixture of three cultured microalgal species: *T-Isochrysis galbana*, *Thalassiosira pseudonana*, and *Chaetoceros muelleri*, at a concentration of 8 million

cells per ml. The amount given to the scallops varied throughout the experiment based on their size and number in each aquarium, ranging from 0.01 L per day in week 5 to 0.43 L per day by week 12. Water quality parameters, including salinity (27–28 ppt), ammonia (0.15 ppm), and pH (8.1–8.3), were routinely monitored. Half of the water volume in each aquarium was changed every other day to ensure optimal conditions. During weeks 12–13, the scallops were fed concentrated refrigerated algae (Shellfish Diet® 1800, Reed Mariculture, CA, USA), which was followed by a mass mortality event and termination of the experiment.

Calcein staining and sampling

To track mineral accretion, scallops from both tanks were stained with calcein, a nontoxic fluorescent dye, every two weeks. Prior to staining, the scallops were starved for 24 hours. The staining solution was prepared by dissolving calcein in seawater and adding it to the aquaria to a final concentration of 100 mg L^{-1}. Scallops were exposed to the calcein-loaded seawater for 7 hours, after which the aquaria were purged of calcein stain through three fresh seawater rinses.

Following the staining procedure, 14 scallops from each aquarium were sampled. Seven scallops were fixed in 70% ethanol, while the other seven were fixed in an aldehyde-based fixative (4% paraformaldehyde and 1% glutaraldehyde in 1 N sodium cacodylate buffer). The staining protocol was adapted from ref. 42.

UV fluorescence imaging

The fluorescence signals of calcein-stained shells were detected using an inverted fluorescence microscope (Leica DMi8) equipped with an ultraviolet light source. Images were captured with a 5× objective lens, using an excitation filter with wavelengths between 460–500 nm and a dichroic mirror at 505 nm. Mosaics of multiple images for each scallop shell were assembled using Dragonfly 3D World 2024.1 software (Comet Technologies Canada Inc., Montreal). Increments in shell growth were determined by measuring the distance between pairs of adjacent fluorescence lines, corresponding to the calcein staining events.

Microcomputed X-ray tomography (μCT)/X-ray microscopy

For 3D measurements, scallop shells fixed in 70% ethanol were analyzed using X-ray microscopy. Five shells from each aquarium, sampled on the last day, were transferred into polystyrene tubes containing 70% ethanol and padded with ethanol-imbibed paper to prevent motion artifacts during scanning. X-ray microscopy was performed using a Zeiss Xradia Versa 520 operating at a voltage of 80 kV and a power of 7 W, with a 0.4× objective, a proprietary LE1 source filter, and a 1 second exposure time across 3001 projections. This set-up provided volumes with a voxel size ranging from 5.9 to 10.8 μm.

Segmentation of scallop shells was conducted using grayscale thresholding in Dragonfly 3D World 2024.1 software (Comet Technologies Canada Inc., Montreal). Shell height (Fig. 1a) was measured using the scale tool in Dragonfly. For relative shell thickness measurements, all shells were normalized to the largest shell from the warmer aquarium (Rose). Specifically, the pixel size (x, y and z spacing) of each shell from Jack and Rose aquaria was adjusted by multiplying it by the ratio of the height of the largest shell from Rose to the height of each specimen. This normalization was intended to ensure that variations in shell

thickness were not influenced by differences in overall shell size, but instead reflected size-independent variation in proportions and intrinsic differences in biomineralization patterns, in response to temperature variation.

The histograms of local shell thickness abundance values were plotted for each specimen, and the frequency distributions were interpolated onto a common x-axis ranging from 0 to 500 units with 250 evenly spaced bins. Linear interpolation was applied to standardize the data, with out-of-range values handled by assigning NaN. The mean and standard deviation of the interpolated histograms were calculated for each group to represent the central tendency and variability. The average profiles of the two temperature groups (23 °C in green and 26 °C in orange) were then plotted, with shaded bands indicating ±1 standard deviation to illustrate the variability within each group.

Mechanical testing

Eight scallops of equal size, harvested at week 11 from each aquarium, were patted dry, and their shell strength, stiffness, and toughness were measured using a universal mechanical testing machine (Cellscale® Univert), with a 50 N load cell. All shells were weighed on a precise balance and placed on the right valve. Flat disks of cork (1 mm thick, 15 mm in diameter) were attached to the stainless-steel compression platens to minimize stress concentrations at the points of contact between the shells and the platen. Displacement-controlled compression was performed until a fracture occurred, and load–displacement curves were exported. Shell stiffness was calculated as the slope of the force–displacement curve, and toughness was determined as the area under the curve. Both strength and toughness were normalized to the corresponding shell weight for comparison.

Scanning electron microscopy

For cross-sectional shell microstructure imaging, the whole shell was embedded in Epon resin after serial dehydration in graded acetone. The embedded shells were cut into two halves longitudinally along the axis of maximum growth with a circular diamond saw. The cut sections were subjected to several polishing steps, with a final polish with 40 nm colloidal silica. Polished specimens were affixed to aluminum mounting stubs with carbon tape and sputter-coated with 10 nm of carbon before imaging at 3 kV in a scanning electron microscope Hitachi FEG-SEM SU8000.

Electron backscattered diffraction (EBSD)

For EBSD analysis, shells were embedded in conductive resin (Technovit 5000) and were cut into two halves longitudinally along the axis of maximum growth with a circular diamond saw which were then polished up to 40 nm. Afterward, samples were sputter-coated with a 10 nm layer of carbon. EBSD was carried out at the same region (near hinge and near growing edge) along sections as the SEM images using a scanning electron microscope Hitachi (FEG)-SEM SU8230 equipped with a Bruker EBSD system (Bruker eFlash EBSD camera with ARGUS forescatter detectors). Diffraction patterns were collected at 0.17 μm step size in high current mode, 20 kV accelerating voltage, and a 100 μm objective aperture. The inverse pole figures and phase images were cleaned and processed using the Oxford Instruments AZtecCrystal software.

Data availability

All data supporting this study are included in the article. No additional datasets were generated or analyzed.

Conflicts of interest

There are no conflicts to declare.

Acknowledgements

References

1 M. Hautmann, Paläontologische Zeitschrift, 2010, vol. **84**, pp. 317–322.

2 D. W. Boyd and N. D. Newell, *Pectinoid Bivalves of the Permian-Triassic Crisis. Bulletin of the AMNH*, no. 227, 1995.

3 FAO, *The State of World Fisheries and Aquaculture 2024*, Report 1020-5489, Rome, Italy, 2024.

4 A. R. Brand, in *Developments in Aquaculture and Fisheries Science*, ed. S. E. Shumway and G. J. Parsons, Elsevier, 2016, vol. 40, ch. 11, pp. 469–533.

5 J. S. Gutsell, *Natural History of the Bay Scallop*, US Government Printing Office, 1931.

6 D. Leavitt, R. Karney and A. Surier, *Biology of the Bay Scallop*, Northeastern Reg. Aquacult. Center, 2010, vol. 213, pp. 1–8.

7 M. Castagna, *Mar. Fish. Rev.*, 1975, **37**, 19.

8 K. Simkiss and K. M. Wilbur, *Biomineralization : Cell Biology and Mineral Deposition*, Academic Press Inc., San Diego, CA, 1989.

9 F. Marin, N. Le Roy and B. Marie, *Front. Sci.*, 2012, **4**, 1099–1125.

10 B. Boggild O, Det Kongelige Danske Videnskabernes Selskabs Skrifter. Naturvidenskabelig og Mathematisk Afdeling, Raekke 9, 1930, vol. **2**, pp. 231–326.

11 D. T. John, W. J. Kennedy and H. Anthony, Bulletin of the British Museum (Natural History). Zoology. 1969, Supplement 3, pp. 1–125.

12 B. Runnegar, *Alcheringa*, 1984, **8**, 273–290.

13 C. Richardson, *Oceanogr. Mar. Biol.*, 2001, **39**, 103–164.

14 T. M. Marchitto, G. A. Jones, G. A. Goodfriend and C. R. Weidman, *Quat. Res.*, 2000, **53**, 236–246.

15 B. D. Stewart, S. R. Jenkins, C. Boig, C. Sinfield, K. Kennington, A. R. Brand, W. Lart and R. Kröger, *Sci. Total Environ.*, 2021, **755**, 143019.

16 P. G. Malone and J. R. Dodd, *Limnol. Oceanogr.*, 1967, **12**, 432–436.

17 S. Milano, B. R. Schöne and R. Witbaard, *Palaeogeogr. Palaeoclimatol. Palaeoecol.*, 2017, **465**, 395–406.

18 W. Satoshi and K. Satoshi, *J. Shellfish Res.*, 2010, **29**, 353–359.

19 T. Okabe and J. Yoshimura, *Sci. Rep.*, 2017, **7**, 42445.

20 D. M. Raup, *J. Paleontol.*, 1966, **40**, 1178–1190.

21 R. R. Stephanie and S. P. Robert, *Am. Malacol. Bull.*, 2021, **38**, 23–33.

22 P. C. Almada-Villela, J. Davenport and L. D. Gruffydd, *J. Exp. Mar. Biol. Ecol.*, 1982, **59**, 275–288.

23 Y. Levi-Kalisman, G. Falini, L. Addadi and S. Weiner, *J. Struct. Biol.*, 2001, **135**, 8–17.

24 F. Nudelman, B. A. Gotliv, L. Addadi and S. Weiner, *J. Struct. Biol.*, 2006, **153**, 176–187.

25 A. Wheeler, in *Calcification in Biological Systems*, CRC Press, 1992, pp. 179–216, DOI: **10.1201/9781003068396-10**.

26 A. R. Palmer, *Mar. Biol.*, 1983, **75**, 287–292.

27 M. Carré, I. Bentaleb, O. Bruguier, E. Ordinola, N. T. Barrett and M. Fontugne, *Geochim. Cosmochim. Acta*, 2006, **70**, 4906–4920.

28 L. W. Hutchins, *Ecol. Monogr.*, 1947, **17**, 325–335.

29 K. R. H. Read and K. B. Cumming, *Comp. Biochem. Physiol.*, 1967, **22**, 149–155.

30 S. J. Gould, *Full House: the Spread of Excellence from Plato to Darwin*, Harvard University Press, 1996.

31 J. M. C. Hutchinson and P. M. Waser, *Biol. Rev.*, 2007, **82**, 335–359.

32 L. Chauvaud, Y. Patry, A. Jolivet, E. Cam, C. Le Goff, Ø. Strand, G. Charrier, J. Thébault, P. Lazure, K. Gotthard and J. Clavier, *PLoS One*, 2012, **7**, e37717.

33 A. J. Lew, C. A. Stifler, A. Tits, C. A. Schmidt, A. Scholl, A. Cantamessa, L. Müller, Y. Delaunois, P. Compère, D. Ruffoni, M. J. Buehler and P. U. P. A. Gilbert, *Adv. Mater.*, 2023, **35**, 2300373.

34 M. Negrini, P. B. Batson, A. M. Smith, S. A. F. Smith, D. J. Prior, H. Henry, K. C. Li and Y. Tamberg, *J. Struct. Biol.*, 2022, **214**, 107882.

35 S. C. Doney, V. J. Fabry, R. A. Feely and J. A. Kleypas, *Annu. Rev. Mar. Sci.*, 2009, **1**, 169–192.

36 O. Hoegh-Guldberg and J. F. Bruno, *Science*, 2010, **328**, 1523–1528.

37 A. M. Stevens and C. Gobler, *Mar. Ecol.: Prog. Ser.*, 2018, **604**, 143.

38 N. Lagos, S. Benítez, C. Duarte, M. Lardies, B. Broitman, C. Tapia, P. Tapia, S. Widdicombe and C. Vargas, *Aquacult. Environ. Interact.*, 2016, **8**, 357.

39 C. L. Mackenzie, G. A. Ormondroyd, S. F. Curling, R. J. Ball, N. M. Whiteley and S. K. Malham, *PLoS One*, 2014, **9**, e86764.

40 P. Abelin, A. Araújo and A. Rombenso, *Current Status of Scallop Culture in Brazil*, 2016.

41 E. Grefsrud, Y. Dauphin, J.-P. Cuif, A. Denis and Ø. Strand, *J. Shellfish Res.*, 2008, **27**, 633–641.

42 L. Wu, L. Zhou, T. Zhang, L. Li, X. Xu, B. Wu, Z. Liu and X. Sun, *Aquac. Rep.*, 2023, **28**, 101463.